

A highly scalable particle tracking algorithm using partitioned global address space (PGAS) programming for extreme-scale turbulence simulations

Dhawal Buaria^{a,b,*}, P.K. Yeung^{b,c}

^aMax-Planck Institute for Dynamics and Self-Organization, D-37077 Göttingen, Germany

^bSchool of Aerospace Engineering, Georgia Institute of Technology, Atlanta, GA 30332, USA

^cSchool of Mechanical Engineering, Georgia Institute of Technology, Atlanta, GA 30332, USA

Abstract

A new parallel algorithm utilizing partitioned global address space (PGAS) programming model to achieve high scalability is reported for particle tracking in direct numerical simulations of turbulent flow. The work is motivated by the desire to obtain Lagrangian information necessary for the study of turbulent dispersion at the largest problem sizes feasible on current and next-generation multi-petaflop supercomputers. A large population of fluid particles is distributed among parallel processes dynamically, based on instantaneous particle positions such that all of the interpolation information needed for each particle is available either locally on its host process or neighboring processes holding adjacent sub-domains of the velocity field. With cubic splines as the preferred interpolation method, the new algorithm is designed to minimize the need for communication, by transferring between adjacent processes only those spline coefficients determined to be necessary for specific particles. This transfer is implemented very efficiently as a one-sided communication, using Co-Array Fortran (CAF) features which facilitate small data movements between different local partitions of a large global array. The cost of monitoring transfer of particle properties between adjacent processes for particles migrating across sub-domain boundaries is found to be small. Detailed benchmarks are obtained on the Cray petascale supercomputer *Blue Waters* at the University of Illinois, Urbana-Champaign. For operations on the particles in a 8192^3 simulation (0.55 trillion grid points) on 262,144 Cray XE6 cores, the new algorithm is found to be orders of magnitude faster relative to a prior algorithm in which each particle is tracked by the same parallel process at all times. This large speedup reduces the additional cost of tracking of order 300 million particles to just over 50% of the cost of computing the Eulerian velocity field at this scale. Improving support of PGAS models on major compilers suggests that this algorithm will be of wider applicability on most upcoming supercomputers.

Keywords: Turbulence, particle tracking, parallel interpolation, Partitioned global address space (PGAS) programming, Co-Array Fortran, one-sided communication

1. Introduction

Many important problems in nature and engineering, such as pollutant dispersion, cloud physics, and the design of improved combustion devices, are closely tied to the motion of discrete entities in a continuous fluid medium in a state of turbulent motion, characterized by disorderly fluctuations in time and three-dimensional (3D) space. Important applications include the role of pollutant dispersion in atmospheric air quality [1], the coalescence of water vapor droplets leading to rain formation [2], and the mixing of chemical species in turbulent combustion [3]. Although effects of particle inertia [4, 5] and molecular diffusion [6, 7] are often present, the predominant physical mechanism underlying these applications is that of turbulent transport via the motion of infinitesimal material fluid elements, known as fluid particles (or passive tracers), which are (from the continuum viewpoint) of zero size and move with the local flow velocity. Effectively, we adopt the Lagrangian viewpoint of fluid mechanics [8–10] from the perspective of an observer moving with the flow. A number of review articles covering various aspects of this broad subject are given by Refs. [11–16].

*Corresponding author. E-mail address: dhawal.buaria@ds.mpg.de

The trajectory of a fluid particle can be obtained by numerical integration of its equation of motion

$$\frac{d\mathbf{x}^+(t)}{dt} = \mathbf{u}^+(t), \quad (1)$$

where $\mathbf{x}^+(t)$ and $\mathbf{u}^+(t)$ denote the instantaneous particle position and velocity respectively. The fluid particle velocity is given by the velocity of the fluid medium at the instantaneous particle position, i.e.

$$\mathbf{u}^+(t) = \mathbf{u}(\mathbf{x}^+(t), t), \quad (2)$$

where $\mathbf{u}(\mathbf{x}, t)$ represents the so-called Eulerian velocity field seen by an observer at fixed locations in space. To follow the particle trajectories it is thus necessary to first calculate the fluid velocity at a set of fixed grid locations, and then to interpolate for the particle velocity based on its instantaneous position and the Eulerian velocity field at a set of neighboring grid points. Since instantaneous velocities are involved, the only reliable computational technique to obtain the Eulerian information required is direct numerical simulation (DNS), where the velocity field is computed numerically according to the Navier-Stokes equations expressing the fundamental laws of conservation of mass and momentum. The value of DNS as a research tool capable of providing massive detail is well established [17, 18].

Turbulence is one of the main science drivers for high-performance computing [19, 20]. A general desire is to reach Reynolds numbers as high as possible, so that the flow physics captured will bear greater resemblance to that in flows encountered in practical applications. The Reynolds number (Re) is a non-dimensional parameter defined as $Re = \mathcal{U}\ell/\nu$, where \mathcal{U} is a measure of the velocity fluctuations, ℓ is a characteristic length scale of large scales, and ν is the kinematic viscosity. A large Reynolds number implies a wide range of scales in both time and space, which in turn requires a large number of time steps and grid points. Depending on the detailed definitions used and scale resolution desired, it can be estimated that the total computational effort for a simulation over a given physical time period increases with Reynolds number at least as strongly as Re^3 [21]. Advances in computing power have enabled simulations in the simplest geometries at 8192^3 [22] and even 12288^3 [23] grid resolution. On other hand, although the basics of particle tracking are well established [24–26], further challenges arise when tracking a large number of fluid particles at such problem sizes. In particular, since the solution domain is distributed over multiple parallel processes, as each fluid particle wanders around, the identities of parallel processes directly involved in the calculation of its interpolated velocity also evolve. Conversely, each parallel process is called upon to contribute to the interpolated velocities of a constantly-evolving collection of fluid particles at each time step. This can lead to a very inefficient communication pattern, with adverse effects on performance and scalability.

In this paper our ultimate goal is to address the issues associated with particle tracking at extreme problem sizes within a massively parallel programming model, with emphasis on challenges that may not arise or be evident at smaller problem sizes. The first decision in the design of any parallel particle tracking algorithm is how the particles are divided among the parallel processes used for the Eulerian DNS. One basic strategy is to assign to each process the same particles at all times. At each time step the process hosting a fluid particle gathers contributions to the interpolated velocity, from all other processes using a global collective communication call — which unfortunately may not scale well at large core counts. A reduction in scalability at large problem sizes [27] is thus not unexpected, which is more problematic in studies of backward dispersion [28, 29] or rare extreme events [22], where a larger number of particles are necessary. To overcome this limitation we have devised an alternative approach where at each time step, a particle is tracked by the parallel process which holds the sub-domain where the particle is instantaneously located. Each process is then responsible for a dynamically evolving instead of a fixed sub-population of particles. The communication required becomes local in nature, occurring (if at all) only between parallel processes holding sub-domains adjacent to one another. This “local communication” approach has some similarities with the spatial decomposition techniques in molecular dynamics applications [30, 31], and has been used for fluid and inertial particles in turbulence simulations as well [32, 33]. In these previous works usually the host process gathers information from its neighbors in the form of so-called “ghost layers” immediately outside the boundaries of each sub-domain, in a manner similar to parallelized finite difference codes. However, use of ghost layers incurs substantial costs in memory and communication, especially when cubic spline interpolation [24] with a stencil of $4^3 = 64$ points is used in conjunction with a domain decomposition based on Eulerian simulation requirements at large process counts.

Our new algorithm reported in this paper is based on the framework of the local communication approach discussed above, but avoids ghost layers completely. Instead, we utilize a partitioned global address space (PGAS)

programming model, namely Co-Array Fortran [34], to fetch the required data directly from remote memory using one-sided communication. In PGAS programming, the memory of all processes is treated as a global memory, but at the same time portions of shared memory will have affinity towards particular processes, thereby exploiting the locality of reference. In addition, latencies for short messages in PGAS programming can be significantly smaller compared to that provided by the standard Message Passing Interface (MPI) library. This makes PGAS models especially appealing in the current work, because the local communication pattern noted above allows the code to benefit from the memory affinity in PGAS, while the message sizes required for interpolation are also small.

While the programming concepts involved are general, in this work we have focused on code performance on the petascale supercomputer *Blue Waters*, which is a Cray system consisting of 22,400 XE6 and 4,220 XK7 nodes operated by the National Center for Supercomputing Applications (NCSA) located at the University of Illinois at Urbana Champaign, USA. We are able to achieve very good performance (with a very large speedup) for our production problem size of 8192^3 grid points on 262,144 Cray XE cores (i.e. 8192 nodes) and up to of order 300 million fluid particles.

The rest of the paper is organized as follows. In Sec. 2 we provide background information on the DNS code which calculates the velocity field, and on our baseline particle tracking algorithm based on a global communication pattern. We also present some performance data for this baseline approach, showing why it is not suitable for simulations at petascale or post-petascale problem sizes. In Sec. 3 we discuss in detail the new parallel implementation which is based on one-sided communication (as opposed to ghost layers) and local communication. In Sec. 4 we provide a performance analysis which shows that, somewhat counter-intuitively, scalability actually improves as the problem size and core count increase. Finally in Sec. 5 we summarize the performance improvements in this work and briefly comment on its potential applicability on the next wave of post-petascale platforms to come. Science results enabled by the new algorithm are to be reported separately.

2. Eulerian setup and base particle-tracking algorithm

While our focus is on tracking particles, efficient calculation of the Eulerian velocity field is a major prerequisite which also drives the overall structure of the DNS code. We thus begin with a brief account of the Eulerian DNS code which calculates the velocity field. We also give a brief account of how cubic spline coefficients are calculated, and of our baseline algorithm in which the mapping between particles and MPI processes is fixed in time.

2.1. Eulerian DNS code structure

In the interest of simplifying the flow geometry but focused on reaching higher Reynolds numbers, we consider stationary homogeneous isotropic turbulence in a 3D periodic domain. The incompressible Navier-Stokes equations expressing conservation of mass and momentum for the velocity fluctuations $\mathbf{u}(\mathbf{x}, t)$ can be written as

$$\nabla \cdot \mathbf{u} = 0 \tag{3}$$

$$\partial \mathbf{u} / \partial t + \mathbf{u} \cdot \nabla \mathbf{u} = -\nabla(p/\rho) + \nu \nabla^2 \mathbf{u} + \mathbf{f}, \tag{4}$$

where ρ is the density, p is the pressure, ν is the kinematic viscosity and \mathbf{f} denotes a numerical forcing term used to sustain the fluctuations [35, 36]. The solution variables are expanded in a Fourier series with a finite number of wavenumber modes. The equations are transformed to wavenumber space, where the divergence-free condition in (3) is enforced by projecting all terms transformed from (4) onto a plane perpendicular to the wavenumber vector. To avoid prohibitively-costly convolution sums associated with Fourier transforms of the nonlinear terms ($\mathbf{u} \cdot \nabla \mathbf{u}$) it is standard to use a pseudo-spectral method [37, 38], whereby the nonlinear terms are formed in physical space and transformed back to wavenumber space. The resulting aliasing errors are controlled by a combination of truncation and phase-shifting techniques [39]. Time integration is performed using an explicit second order Runge-Kutta method, where a Courant number (C) constraint of $C < 1$ is required for numerical stability.

Clearly, the feasibility of high-resolution pseudo-spectral DNS is highly dependent on the parallel implementation of 3D FFTs, which are of general interest in themselves [40–43]. Our Eulerian code base is thus designed to make the 3D FFTs as efficient as possible. We consider the case of N grid points in each direction. The simplest domain decomposition scheme is one-dimensional (1D), such that each process holds one “slab” of data, of size $N \times N \times N/P$,

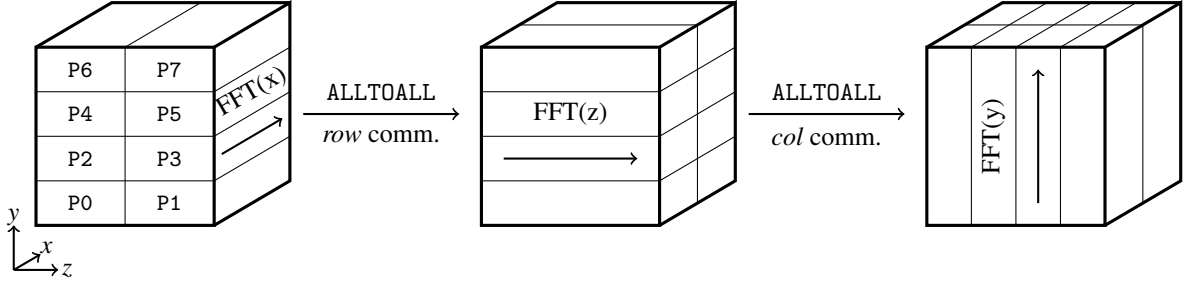


Figure 1: A schematic showing the 2D domain decomposition and transposes required for the 3D-FFT. For simplicity, we show the case of 2×4 processor grid with 8 parallel processes labeled P0 to P7.

where P is the number of MPI processes. This method is obviously restricted to $P \leq N$, which is less appealing on very large systems unless OpenMP multithreading is highly effective. Instead we use a 2D decomposition, such that each process holds a “pencil” of data, of size $N \times N/P_r \times N/P_c$, where $P_r \times P_c = P$ defines the 2D Cartesian process grid geometry. In this setup, there are P_c row communicators of size P_r each, and likewise P_r column communicators of size P_c each [40]. The schematic in Fig. 1 illustrates the sequence of operations for a 3D real-to-complex transform, beginning with pencils of data in the first (x) direction. The 1D FFTs in each direction are taken using the FFTW software library, with data in the local memory, while transposes using ALLTOALL collective communication within row or column communicators are used to re-align pencils of data along the required directions. Because data involved in the communication calls reside in non-contiguous areas of memory, some local transpose (pack and unpack) operations are also required. To facilitate fast arithmetic we use stride-one arrays whenever possible.

Pseudo-spectral codes tend to be communication intensive. We have found it beneficial to let P_r be small compared to P_c , with P_r matching (or less than) the number of cores on a node (say P_{node}), such that the ALLTOALL within the row communicator can occur entirely on the node, bypassing the slower interconnect. For example, on *Blue Waters* with $P_{node} = 32$, we have performed 8192³ simulations on a 32×8192 processor grid. We also use a PGAS implementation (based on Co-Array Fortran) to perform the ALLTOALLs [44], whereby remote-memory access (RMA) is utilized by declaring global co-arrays as buffers to perform the required communication. The use of such RMA based programming, typically utilizing MPI-3 or PGAS models, to improve collective communication costs, is becoming increasingly widely adopted [45, 46].

While the communication costs are greatly reduced by using these strategies, the choice of $P_r \leq P_{node}$ means that P_c must be made larger as P increases, with N/P_c ultimately becoming as small as unity. As we will see later, this feature has special implications for our new particle tracking algorithm.

2.2. Cubic-spline coefficients and baseline particle tracking algorithm

Several different interpolation schemes have been used in the literature [24, 26, 32, 33] to obtain particle velocities in turbulence simulations. A scheme of high order of accuracy is important, especially if one wishes to compute velocity gradients (which are less well-resolved in space) following the particle trajectories as well [47, 48]. In addition, the study of fluid particle acceleration [49, 50], which is obtained by differentiating the velocities in time, requires that the interpolated functions be smooth in space. These requirements are well met by cubic-spline interpolation, which is fourth-order accurate and (in contrast to piece-wise polynomials) twice differentiable.

Suppose at any given time step, a fluid particle is located within a grid cell labeled by the integer indices α, β, γ such that $x_\alpha \leq x^+ \leq x_\alpha + \Delta x$, $y_\beta \leq y^+ \leq y_\beta + \Delta y$, and $z_\gamma \leq z^+ \leq z_\gamma + \Delta z$, with uniform grid spacings $\Delta x, \Delta y, \Delta z$; and S_{pqr} with $1 \leq p, q, r \leq N + 3$ are the cubic spline coefficients for a flow variable $g(\mathbf{x})$ in 3D space. The interpolated value of g at the particle position is given by

$$g^+ = \sum_{k=1}^4 \sum_{j=1}^4 \sum_{i=1}^4 b_i(x') c_j(y') d_k(z') S_{pqr}, \quad (5)$$

where $p = \alpha + i - 2$, $q = \beta + j - 2$, $r = \gamma + k - 2$; primes indicate normalized local coordinates, such as $x' = (x^+ - x_\alpha)/\Delta x$; and $\{b_i\}$, $\{c_j\}$ and $\{d_k\}$ are 1D basis functions in x, y, z directions respectively. The latter are of compact support over an

interval of four grid spacings only and have the same prescribed functional forms as in Ref. [24]. Periodic boundary conditions for the particle velocities are enforced by recognizing that the velocity of a particle located outside the primary domain of length L_0 on each side (usually $L_0 = 2\pi$) is the same as if it were at a “shadow” location inside the primary domain shifted by multiples of L_0 in each direction. For each particle, use of the interpolation formula above requires three major operations, which we refer to as (1) generation of spline coefficients based on the velocity field; (2) evaluation of basis functions based on the particle position; and (3) summation over $4^3 = 64$ contributions.

The first of these three operations is Eulerian in nature and independent of the other two, as well as the number of particles tracked. Similar to FFTs, the spline coefficients are partitioned using a 2D domain decomposition and operated on one direction at a time, in the ordering x, z, y as suggested in Fig. 1. Along each grid line of N grid points we determine $N + 3$ coefficients by solving a tridiagonal system of simultaneous equations [51] with periodicity in space. Transposes between pencils of partially-formed spline coefficients are also required. However since $N + 3$ is not divisible by P there is a slight imbalance in the message sizes that each MPI process sends and receives. Consequently the transposes are implemented by ALLTOALLV constructs which allow for non-uniform message sizes. On *Blue Waters* an improvement in performance is obtained by using a Co-Array Fortran equivalent of ALLTOALLV [44]. In addition, operations needed to solve spline equations in the y and z directions are subject to a non-unity vector stride and are hence slower than that in the x direction, while the packing and unpacking operations are also less efficient than those used for 3D FFTs on an N^3 array. For these reasons, overall the operation of forming the spline coefficients scales less well than 3D FFTs, and the cost of generating the spline coefficients may be substantial. However, this cost is a necessary expense if differentiability of the interpolated results is important.

Operations 2 and 3 as listed above are dependent on how information on the particle population is divided among the MPI processes. The baseline version of our algorithm uses a static-mapping approach where (as noted in Sec. 1) each MPI process is responsible for the same particles at all times. The total population of N_p particles is divided into P sub-populations of size N_p/P each. Initially, each sub-population of particles can be distributed randomly either within its host sub-domain, or throughout the solution domain, with coordinates between 0 and L_0 . The latter is convenient for post-processing, where each sub-population of particles can be taken as a single realization for ensemble averaging. Statistical independence between these sub-ensembles is achieved by a different random number seed for each MPI process when calling Fortran intrinsic random number generator (RANDOM_NUMBER) to initialize the particle positions.

Operation 2 can now be carried out readily on each MPI process, since the 1D basis functions (b_i, c_j, d_k) are simple algebraic functions of the reduced particle position coordinates (x', y', z' , which are already known to the MPI process). However in preparation for Operation 3, information on local particle coordinates (the quantities $\alpha, \beta, \gamma, x', y', z'$ used in (5)) for all particles must be made available to all MPI processes. This information sharing can, in principle, be implemented through a global MPI_ALLGATHER collective communication call, which however scales very poorly at large P . Alternatively, to reduce the number of MPI processes engaged in collective communication we can use a hierarchical approach based on a row-and-column communicator of dimensions say $P_1 \times P_2$ (which are distinct from P_r and P_c used in the rest of the code). This scheme consists of an MPI_GATHER first used to collect data within each row, followed by an MPI_ALLGATHER across a column, and finally a MPI_BCAST (which can be implemented using non-blocking MPI_ISEND and MPI_RECVs) back within each row. Since only one lead process from each row needs to participate in the MPI_ALLGATHER a substantial improvement is achievable by using a small P_2 . Both a standard MPI_ALLGATHER and its hierarchical version require additional storage, which is in principle proportional to the number of particles but can be reduced by dividing the N_p particles into several batches and operating on each batch sequentially.

After the MPI_ALLGATHER communication above, each MPI process is now able to participate in Operation 3 by calculating its own partial contributions to the summation in (5) for all particles. This task requires collecting and adding partial sums collected from different MPI processes and subsequently returning to each MPI process the results for the particles that it is responsible for. In principle these data movements can be accomplished by using a combination of MPI_REDUCE and MPI_SCATTER between all processes. However, we have also used CAF to implement this REDUCE+SCATTER using a binary-tree communication pattern [27], whereby processes exchange information with each other in pairs over $\log_2 P$ cycles. By using smaller message sizes, similar to CAF implementation of ALLTOALL [44], the one-sidedness of the tree-based CAF implementation allows for significant reductions in latency costs, thereby offering significant speedup over its MPI counterpart.

Since the operations in the two preceding paragraphs are communication-sensitive, in the search for improved

scalability we have also considered use of OpenMP multi-threading [27]. In the hybrid MPI-OpenMP programming model, it is best to use a configuration such that the product of P_r and the number of threads per MPI process (n_{thr}) is equal to the number of cores available per node. To avoid memory-access penalties across different NUMA domains, P_r can be set equal to the number of NUMA domains available on each node, with all threads associated with a given MPI process placed within the same NUMA domain. The DNS code in our work is actually completely hybridized for simultaneous use of MPI and OpenMP. A reduction of the number of MPI processes does lead to better performance for Operations 2 and 3 via a reduced costs in latency associated with large process counts. However on *Blue Waters* OpenMP appears to be much less competitive when used together with Co-Array Fortran, and the generation of spline coefficients does not benefit from multi-threading. Accordingly, we present only single-threaded timings here.

As might be expected, for a given problem size, the performance of the approach described here depends on the number of MPI processes, the communication performance of the machine used, as well as the availability of a robust Co-Array Fortran implementation. Because of a heavy reliance on global communication over many parallel processes, it is not surprising that scalability is not sustained well at large problem sizes.

Grid points (N^3)	2048 ³	4096 ³	8192 ³	2048 ³	4096 ³	8192 ³
CPU cores (P)	4096	32768	262144	4096	32768	262144
Proc. Grid ($P_r \times P_c$)	32x128	32x1024	32x8192	32x128	32x1024	32x8192
No. particles (N_p)	16M	16M	16M	64M	64M	64M
Eulerian (3D-FFTs)	4.60	6.59	9.20	4.60	6.59	9.20
Weak scaling %	–	76.1%	77.6%	–	76.1%	77.6%
Spline coefficients	1.66	2.33	4.42	1.66	2.33	4.42
Weak scaling %	–	71.2%	52.7%	–	71.2%	52.7%
Allgather (global)	0.71	2.89	7.69	2.83	11.32	29.57
Allgather (hierarchical)	0.70	1.03	1.35	2.99	4.73	5.58
Computations	0.40	0.39	0.39	1.68	1.59	1.60
Reduce+Scatter (CAF)	0.83	1.52	2.94	4.14	8.32	11.34
Particles total	1.93	2.94	4.68	8.65	14.64	18.52
Interpolation total	3.59	5.27	9.10	10.31	16.97	22.94

Table 1: Performance data obtained on *Blue Waters* using the static particle-to-process mapping in our baseline algorithm for $N_p=16M$ (left columns) and 64M (right columns) particles (where $M = 2^{20} = 1,048,576$). The timings shown are elapsed wall time per second-order Runge Kutta time step, to the nearest hundredth of a second. Weak scaling is calculated for each doubling of N , with the number of operations being proportional to $N^3 \log_2 N$ for the Eulerian code and N^3 for the calculation of spline coefficients. The “particles total” entry is the sum of Allgather (hierarchical), computations and reduce+scatter (using CAF). The “Interpolation total” entry is the sum of “particles total” and spline coefficients.

Table 1 gives a brief summary of performance data for the baseline algorithm. The data are collected by, as usual, measuring the time elapsed between suitably-placed `MPI_WTIME` calls, for the slowest MPI process but taking the best timing over a substantial number of time steps or iterations. For each value of N_p , the Eulerian problem size is varied from 2048³ to 8192³, while the number of MPI processes (P) is varied in proportion to N^3 . We also report weak scaling over each doubling of N , considering the differences in operation counts for 3D FFTs and for the calculation of spline coefficients (based on the solution of tridiagonal systems using the well-known Thomas algorithm). The last row of the table is the sum of all contributions to the cost of interpolation, including generation of spline coefficients, hierarchical allgather, computation, and the tree-based Co-Array Fortran implementation of `REDUCE+SCATTER` for assembling results for all particles and re-distributing them back among the MPI processes.

The Eulerian parts of the code have been optimized aggressively in support of recently published work that did not involve fluid particles [22]. About 77% weak scaling is obtained for each doubling of N . As suggested earlier in this subsection the calculation of spline coefficients scales less well while being also independent of N_p . In subsequent rows of the table the timings are generally proportional to N_p . A global `MPI_ALLGATHER` over all MPI processes is seen to perform very poorly, with roughly a factor of 3 increase in cost between successive problem sizes. The hierarchical scheme performs much better but its scalability is also not good, considering that it takes longer even as the number of particles per MPI process decreases by a factor of 8 between adjacent columns of the table with N_p held fixed. Scalability measures of the computational operations in (5) and subsequent communication needed to complete

the interpolation are also evidently far from ideal.

Since our science objectives call for a simulation with $N = 8192$ and (at least) $N_p = 256M$, four times more than the largest N_p shown in Table 1, it is clear that a new approach for the particle tracking algorithm is required.

3. Dynamic particle-to-process mapping and local communication

As indicated earlier (Sec. 1), to reduce communication costs in interpolation it is helpful to divide the particle population among the MPI processes according to a dynamic mapping based on instantaneous particle positions, such that at each time step each particle is processed by the MPI process that holds the sub-domain where the particle is located. If the interpolation stencil (of 64 points for cubic splines) surrounding the particle position lies wholly within the sub-domain then no communication is needed. Otherwise, for particles located close to the sub-domain boundaries, communication is still required to access some of the spline coefficients held by one or more neighboring MPI processes. However, in contrast to the global communication pattern in the baseline algorithm (Sec 2.2) these communications will now be local, occurring only between pairs of MPI processes holding sub-domains next to each other. In principle, information from neighboring MPI processes can be obtained through the concept of ghost layers, which is common in parallelized finite difference schemes but (as explained below) is not ideal for our application. Instead we have devised a new communication protocol based on one-sided communication via Co-Array Fortran (CAF), which is advantageous on *Blue Waters* and likely to be more widely available in the future.

An inherent feature of the dynamic particle-to-process mapping is that, as particles cross the sub-domain boundaries, control for the migrating particles needs to be passed from one host MPI process to another. Since the number of particles tracked by each MPI process now changes dynamically at every time step, some transient load imbalance is anticipated. However, since in homogeneous turbulence the spatial distribution of particles is statistically uniform, this imbalance is expected to be minor, as long as the average number of particles per MPI process is large ($N_p/P = 1024$ in our largest simulation). At the same time, only particles already located very close to the sub-domain boundaries can possibly migrate, and the likelihood of such migrations is proportional to the time step size (Δt). In our simulations, for reasons of numerical stability and temporal accuracy, we choose Δt such that the Courant number to be 0.6 — which means no fluid particle can travel more than 0.6 grid spacing in any coordinate direction over one time step. This constraint is expected to help reduce the communication overhead for the inter-process migrations.

The principle of ghost layers is that each parallel process extends its reach by accessing several layers of information along the boundary with a neighboring parallel process, while also providing similar information to the latter. The communication is generally of the SEND+RECV, or halo type. Spline coefficients in these ghost layers will have to be refreshed — via communication — at every Runge-Kutta sub-step. Since spline coefficients are stored in a 2D domain decomposition, each MPI process will be performing these halo exchanges with four of its neighbors (two in each direction where the domain is sub-divided). For cubic splines these ghost layers must also be three points deep on each side. For an N^3 problem with $(N + 3)^3$ spline coefficients on a $P_r \times P_c$ processor grid, since $N + 3$ is not divisible by P_r or P_c , each parallel process needs to hold up to $(N + 3)(N/P_r + 1)(N/P_c + 1)$ of the coefficients. If ghost layers are included this increases to $(N + 3)(N/P_r + 6)(N/P_c + 6)$ based on the considerations above. The consequent increase in memory requirements may be mild if both N/P_r and N/P_c are large numbers (being least if $P_r \approx P_c \approx \sqrt{P}$), but very substantial if one of them is small. However at large problem sizes in the DNS, FFT and Eulerian code performance favors processor grids where $P_c \gg P_r$. In our 8192^3 simulation $P_r = 32$ and $P_c = 8192$, such that N/P_c is as small as unity. This implies a memory increase by a factor of at least $(1 + 6)/(1 + 1) = 3.5$, which will likely require using even more cores and thus make the simulations more expensive.

In addition to memory, the size of the ghost layers also has a direct effect on the volume and cost of the communication traffic involved in the halo exchanges. However, each spline coefficient in those ghost layers will be actually used for interpolation only if there is at least one particle in the pertinent immediate neighborhood. The probability of such an occurrence is proportional to the number of particles per grid point, i.e. the ratio N_p/N^3 , and the fraction of particles located within three grid spacings of the sub-domain boundaries. Although in general the number of particles needed for reliable sampling increases with Reynolds number [13, 28], in most simulations N_p is much smaller than N^3 . Indeed, in our 8192^3 simulation even with N_p in the order of 3×10^8 , the ratio N_p/N^3 is still less than 0.001. Furthermore, with N/P_r being large, the fraction of particles that actually require spline coefficients in the ghost layers extending in the direction of the row communicator is expected to be small. Consequently, in contrast to finite difference calculations, for our application both the memory and communication costs of having the complete ghost

layers are very wasteful. The effects of additional memory may be less severe if we use a 3D domain decomposition, since then no individual dimension of the 3D sub-domains will be particularly small. However this will prevent FFTs from being taken in core, and hence would adversely affect the performance of the Eulerian portions of the code.

To scale effectively to extreme problem sizes, we have designed a new algorithm that avoids ghost layer completely, while associating each particle dynamically with the MPI process that holds the sub-domain where the particle resides. To avoid the wastefulness of unused spline coefficients in the ghost layers we transfer spline coefficients between neighboring parallel processes only on an as-needed basis. This is achieved by examining the position of each particle, and deciding (based on the proximity of the particle to sub-domain boundaries), whether any (and how many) spline coefficients are needed from neighboring MPI processes. The host MPI process for the particle then fetches only those specific coefficients, directly from remote memory using one-sided communication. After this task the host process is now able to complete the interpolation for the particle velocity and calculate updated position coordinates. If a particle has migrated to an adjacent sub-domain a one-on-one halo exchange is also used to transfer the control of the particle to its new host MPI process.

The key to the performance of this new algorithm is obviously in how the one-sided communication is performed. For each particle, the 64 spline coefficients needed are either available in the local memory or fetched from the remote memory and stored in a temporary array. To fetch the spline coefficients efficiently, we use a partitioned-global address space (PGAS) programming model, such as Co-Array Fortran (CAF). Essentially, the entire memory space of all the processes is treated as a global memory, partitioned logically such that a portion of it is local to each MPI process. However, (as noted in Sec. 1) depending on the physical proximity to the memory of each process, portions of the shared memory space may have an affinity for a specific parallel process. This suggests the memory locality of the data can be exploited for further optimization. In CAF, which is well supported on *Blue Waters*, the PGAS model is implemented by declaring global co-arrays, which have an additional co-dimension (denoted by square brackets, distinct from the usual parentheses for regular arrays), which allows any MPI process to access information held by other processes. Compared to MPI, communication calls in CAF can (due to one-sidedness) have smaller headers and therefore can carry more data per packet for slightly higher bandwidth. Latencies for short messages in CAF are also significantly lower than in MPI. Thus CAF is perfectly suited for current application, since the messages for individual particles are small. The performance improvement from PGAS programming is well known for many applications ranging from tuning of collective communication calls [44, 46] to molecular dynamics simulations [52].

Our strategy of using CAF for the interpolation is illustrated by a pseudo-code shown in figure 2. We begin at a stage in the calculation where the Eulerian velocity field at N^3 grid points is available as pencils sub-divided in the y and z directions. The array containing the spline coefficients is declared as a global array, called `spline_coarray`. The last dimension of this array, in square brackets, is the co-dimension, which is the same as the rank (0 to $P - 1$) of each of the P MPI processes used. As noted in Sec. 2.2, the spline coefficients are calculated by solving a tridiagonal system of equations in each direction, with a total of two ALLTOALLV transposes in between, one for each of the row and column communicators. The code then enters the main interpolation section which loops over all the particles. For each particle we map its position coordinates to indices α, β, γ and the normalized local coordinates x', y', z' that together allows the basis functions required in (5) to be calculated. This mapping is direct and simple, but also accounts for particle positions outside the primary domain of dimensions L_0^3 , through a modulo function which gives a corresponding position inside the primary domain by adding or subtracting a multiple of L_0 in each direction.

The most important use of CAF in our algorithm is to fetch the spline coefficients required by each particle. For each particle the code loops over the four (with the indices j and k from 1 to 4) basis functions in each of the y and z directions. For each choice of j and k , the code calculates the rank (denoted by `target_rank`) of the MPI process holding the spline coefficients required. If a particle is lying in the interior (at least four grid spacings from the boundary) of the sub-domain of its host MPI process then `target_rank` would be the same as the rank of the host process. Otherwise, it will be the rank of one of the neighboring processes, from which some spline coefficients are to be fetched, along with corresponding local indices. In each case the spline coefficients are to be transferred in packets of four, covering all information needed in the x direction (which is not sub-divided). The message size in each CAF memory copy operation is thus very small (4 floating-point words), for which CAF usually performs best. The co-array language syntax is very convenient, in that if the `target_rank` as shown in figure 2 is the same as the rank of the local MPI process, then the CAF assignment operation functions as a local memory copy; otherwise, a one-sided communication is performed to fetch the required information from the global memory. The `target_rank` process is always a neighbor of the host MPI process, which allows us to further exploit the memory locality of the

```

1  ! N = no. of grid points in each direction; p_row x p_col = proc. grid
2
3  ! spline coefficients are declared in a global co-array
4  ALLOCATE ( spline_coarray (N+3, N/p_row + 1, N/p_col + 1) [p_row*p_col] )
5  ! calculate the spline coefficients
6  CALL calculate_spline_coefficients (spline_coarray)
7
8  ! loop over all particles and perform the interpolation
9  ! num_particles = particles held by a given MPI process
10 loop_ip: DO ip = 1, num_particles
11
12     posn_ip = x-y-z coordinate of particle ip
13     ! the basis functions are calculated using particle co-ordinate
14     (bx(1:4), cy(1:4), dz(1:4)) = calculate_basis_functions (posn_ip)
15
16     ! the particle position is mapped to a integer location on the grid
17     ! ix,iy,iz corresponds to alpha, beta, gamma in eqn-5
18     (ix,iy,iz) = map_posn_to_starting_global_index (posn_ip)
19
20     ! domain is divided in y and z directions with pencils aligned in x
21     loop_k: DO k=1,4
22         loop_j: DO j=1,4
23
24             ! figure out the rank of the MPI process based on j,k indices
25             target_rank = map_array_indices_to_rank (iy+j,iz+k)
26             ! the array index on the target rank
27             ! (if target rank is same as the local rank then iy_loc = iy+j and iz_loc=iz+k)
28             iy_loc, iz_loc = array_indices_based_on_target_rank (iy+j,iz+k)
29             ! the communication call using co-array fortran
30             spline_temp(1:4) = spline_coarray (ix+1:ix+4, iy_loc, iz_loc)[target_rank]
31             ! calculate the final summation
32             loop_i: DO i=1,4
33                 velocity_ip = velocity_ip + bx(i)*cy(j)*dz(k)*spline_temp(i)
34             ENDDO loop_i
35
36         ENDDO loop_j
37     ENDDO loop_k
38
39 ENDDO loop_ip

```

Figure 2: Pseudo-code showing an outline of the sequence of operations in cubic spline interpolation based on a spatial decomposition of particles and local communication implemented using Co-Array Fortran. Fortran syntactical elements are in red; descriptive comments are in blue.

co-array, thus achieving fast and efficient communication. After this communication is complete the summation over 64 basis functions and spline coefficients in (5) is performed entirely by the host process for each particle.

Before proceeding to the performance results in the next section (which shows very favorable performance for our CAF-based approach), it is worth noting that there may be some applications where the ghost layer approach may prevail instead. The ghost layer approach is bandwidth-bound, with communication cost proportional to the number of grid points (N^3); while the CAF approach is latency-bound, with cost proportional to the number of particles (N_p). If the particle density is very high i.e. $N_p \gtrsim N^3$, then the CAF approach would be inefficient since it will likely be fetching the same spline coefficients multiple times without recognizing that they can be fetched just once and re-used. However in most turbulence simulations (including ours), the motivation for large N_p comes from statistical sampling, and a very high particle density would imply many particles being initially close together and thus not acting as independent samples. As a result, even although a larger N_p is desired at large N , the ratio N_p/N^3 is very small; in fact smaller at larger problem sizes (in our largest production science work at 8192^3 resolution with 256 M particles the ratio is as small as $1/2048$). Consequently, we anticipate our CAF would be well suited for traditional particle-tracking turbulence simulations. and less so if a very high particle density is required for other science reasons (such as, perhaps, the study of sandstorms with inertial particles).

4. Performance and scalability analysis

In this Section we present performance and scalability data for our latest particle tracking algorithm. During our recent work, the *Blue Waters* machine noted earlier was the only platform of sufficient capacity available to us to support production simulations at 8192^3 resolution. Co-Array Fortran is at present particularly well supported in the Cray Compiling Environment. For these reasons we discuss here performance on *Blue Waters* only, while also hoping to provide a reference point for other comparisons in the future.

Since our application is entirely CPU based, we use only the XE6 nodes which provide 32 cores per node. The compute nodes are interconnected with a 3D torus network topology using the Cray-Gemini interconnect. The communication performance of the code on *Blue Waters* also benefits substantially from availability of Topologically Aware Scheduling, which attempts to assign to a user’s job a set of nodes with more favorable network topology less prone to network contention from other jobs running concurrently on the system. [44]. Clearly, the time taken at each time step depends on the number of grid points (N^3), the number of particles (N_p), the number of MPI processes (P), and the shape of the processor grid ($P_r \times P_c$) used for 2D domain decomposition. While certain parts of the particle tracking algorithm can be timed via a separate kernel, the actual communication traffic in the algorithm of Sec. 3 is to some degree sensitive to the time evolution of the flow physics itself. We thus report per-step timings directly from the production DNS code, by averaging over a large number of time steps. This averaging also indirectly absorbs the long-term effects of variability due to random factors such as network contention.

In the subsections below we consider separately code performance for generating cubic spline coefficients, using them to obtain interpolated particle velocities, managing the inter-process transfer for particles migrating between adjacent sub-domains; and, ultimately, the total simulation time per time step up to 256 M particles on a 8192^3 grid.

4.1. Calculation of spline coefficients

The calculation of $(N + 3)^3$ spline coefficients from the velocity field known at N^3 grid points shares some similarities but also some significant differences with the Eulerian 3D FFT operations. The similarities include operating one direction and a time, using a 2D domain decomposition, and the need for transposes along each of the sub-divided directions. The optimal shape of the 2D processor grid is also likely to be the same as that for the 3D FFTs. Along each direction, instead of FFTW we solve a tridiagonal system of equations whose operation count scales with N . The dominant cost is communication, while local packing and unpacking also takes significant time. However, because $N + 3$ is not divisible by P_r nor P_c the data structure for spline coefficients is more intricate. In contrast to the FFT routines the arithmetic here is performed with unit stride only in the x direction, while operations along y and z have vector strides proportional to N and N^2/P_r respectively.

N	2048	2048	2048	4096	4096	4096	8192	8192
P	2K	4K	8K	16K	32K	64K	128K	256K
$P_r \times P_c$	32×64	32×128	32×256	32×512	32×1024	32×2048	32×4096	32×8192
x	0.152	0.071	0.036	0.152	0.077	0.035	0.153	0.076
y	0.290	0.149	0.075	0.309	0.149	0.075	0.321	0.160
z	0.327	0.160	0.081	0.520	0.251	0.139	0.894	0.453
pack+unpack	0.281	0.143	0.076	0.281	0.144	0.070	0.290	0.149
alltoallv1	0.560	0.365	0.206	0.562	0.374	0.144	0.611	0.381
alltoallv2	1.349	0.761	0.496	1.976	1.303	0.828	4.181	3.215
total	2.990	1.664	0.977	3.837	2.332	1.310	6.449	4.422
%comm.	63.8%	67.7%	71.9%	66.1%	71.9%	74.2%	74.3%	81.3%
strong	–	89.9%	76.5%	–	82.2%	73.2%	–	72.9%
weak	–	–	–	77.9%	71.3%	74.5%	46.4%	37.6%

Table 2: Elapsed wall time for the calculation of spline coefficients including a breakdown into several sub-contributions as discussed in the text. In the leftmost column x, y, z represent time for calculating 1D spline coefficients in the respective directions. Communication costs for transposes in the row and column communicators are in rows labeled by *alltoallv1* and *alltoallv2* respectively. (Note K denotes $2^{10} = 1024$.)

Table 2 shows the costs of various sub-operations in the calculation of the spline coefficients, for problem sizes 2048^3 , 4096^3 and 8192^3 . For each choice of N the core count P is varied over a factor of up to 4, with P_r fixed at 32

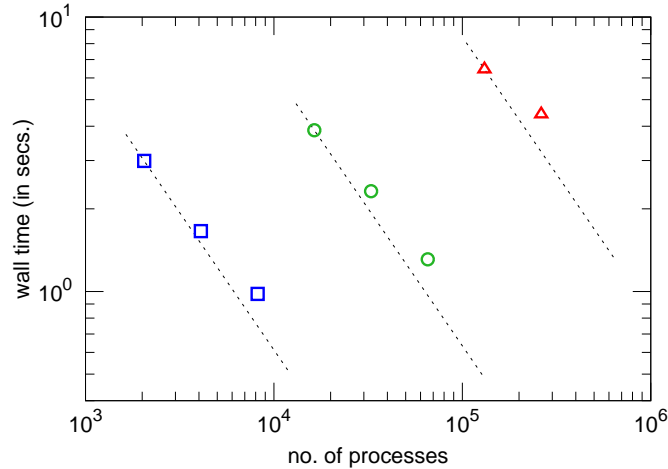


Figure 3: Elapsed wall time for calculation of spline coefficients, versus core count (P) for problem sizes 2048^3 (□), 4096^3 (○), 8192^3 (△). Dashed lines of slope -1 on the logarithmic scales represent ideal strong scaling with respect to case of smallest P for each problem size.

(the number of cores available on each *Blue Waters* node). Because of differences in the striding, operations in the x direction are fastest, followed with those in y and z , especially at larger problem sizes. As the core count P increases, essentially perfect strong scaling is observed for these 1D operations as well as the memory copies (packing and unpacking). The most expensive operations are the transposes (coded as ALLTOALLVs), The first transpose is faster since it takes place in a smaller communicator on the node, whereas the second is slower since it has to be routed through the network interconnect. The percentage of time spent in communication also increases with both problem size and core count, leading to a gradual reduction of scalability.

Figure 3 shows the timings versus core count, on logarithmic scales where perfect strong scaling would be indicated by a line of slope -1, while perfect weak scaling would be indicated by wall time being constant if P is varied in proportional to N^3 . In general for a given problem size, as core count is increased, the data points increasingly deviate from the ideal strong scaling. The percentages of strong scalability shown are slightly lower than that usually achieved for 3D FFTs under similar conditions. The departure from perfect weak scaling is evidently more pronounced, especially at 8192^3 . It is possible that aggressive use of OpenMP multithreading with dedicated threads for communication [53] may lead to some improvements in the future. However, as shown later in the paper the overall scalability of our new parallel algorithm is still good.

4.2. Interpolation operations for particles

With spline coefficients obtained as above, the cost of the remainder of the interpolation operations is expected to scale with the number of particles (N_p). However, actual timings (with N_p fixed) still show sensitivity to the Eulerian problem size and its associated 2D domain decomposition. These effects are felt through the cost of memory access to larger arrays of spline coefficients, and — more importantly — the need for communication between adjacent MPI processes for particles lying close to the sub-domain boundaries. The last of these effects is the most subtle and requires careful discussion, as given in a later part of this subsection.

For an overview of interpolation performance we show in Fig. 4 the elapsed wall time taken by the loop `loop_ip` in the pseudo code presented earlier in Fig. 2. Since the efficiency of Eulerian operations is still important, we consider the same grid resolutions and core counts (along with the processor grid) as those discussed earlier in Sec. 4.1. For each combination of N and $P_r \times P_c = P$ we have obtained timings for $N_p = 16M, 64M$ and $256M$, represented by symbols of different shapes for each color. It can be seen that, with N fixed (considering symbols of a given color), strong scaling with respect to N_p as P increases is less than perfect. However this strong scaling improves with grid resolution: e.g. with N_p fixed the timing for $N = 4096$ and $P = 16384$ is almost exactly half of that for $N = 2048$ and $P = 8192$. More significantly, the best strong scaling with respect to P (with both N and N_p fixed) occurs at the largest N , which can be seen in the positions of symbols in red relative to dashed lines of slope -1 in the figure. These

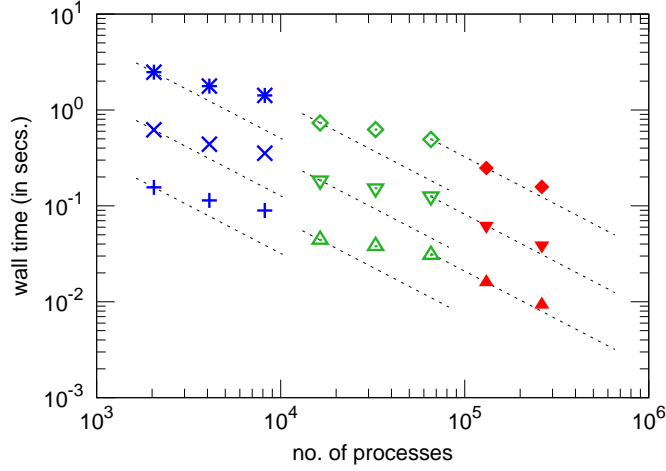


Figure 4: Elapsed wall time for the interpolation operation using the dynamic particle-to-process mapping at grid sizes of 2048^3 (+, ×, *), 4096^3 (△, ▽, ◇), 8192^3 (▲, ▼, ◆), where the three symbols for each grid size corresponds to 16M, 64M and 256M particles respectively ($M = 1, 048, 576$). Dashed lines of slope -1 represents ideal strong scaling with respect to first case of each problem size.

trends are seen to hold uniformly for all three values of N_p tested, with all timings in the figure being proportional to N_p . We explain these trends below by analyzing the effect of the grid resolution and processor grid geometry when employing the dynamic particle-to-process mapping described in Sec. 3.

The elapsed wall times shown above can be separated into contributions from computation and communication, which we denote by t_{comp} and t_{comm} respectively. The computation carried out by each MPI process is to determine the local coordinates and perform the summation in (5) for each particle that is held by that process at the beginning of a time step. This implies t_{comp} is, in principle, proportional to the number of particles per process, i.e. N_p/P , or at least will increase systematically with N_p but decreases with P . Because the turbulence in our simulations is homogeneous, the distribution of particles is spatially uniform. Consequently, although particle migrations between adjacent sub-domains occur on a regular basis, the number of particles carried by each MPI process is expected to deviate only slightly from the averaged value (N_p/P).

The communication time t_{comm} is, in contrast, directly related to the number of particles for which communication is required to access at least some of the spline coefficients. Referring back to the pseudo-code in Fig. 2 the key is how many times that the `target_rank` is not the same as the rank of the host MPI process. The likelihood of such occurrences is in turn tied to the fraction of (on average) N_p/P particles per MPI process that happen to be located within some Γ grid spacings from the sub-domain boundaries. (If a particle lies outside the domain itself we use a corresponding “shadow” position that is inside the solution domain and hence inside one of the sub-domains.) Since cubic spline interpolation requires 4 points in each direction we may take $\Gamma = 2$ (half of 4). In our 2D domain decomposition, each sub-domain is nominally a pencil: a cuboid measuring N , N/P_r and N/P_c grid spacings in the x, y, z directions respectively. Each sub-domain has four rectangular faces in contact with its neighbors: two each of dimensions $N \times N/P_r$ and $N \times N/P_c$ respectively. The volume of the region where particle positions can lead to a requirement for communication is thus equal to $2\Gamma(N \times N/P_r + N \times N/P_c)$ grid cells. Since in homogeneous turbulence the particles are uniformly distributed in space we can estimate

$$t_{comm} \propto 2\Gamma \frac{N \times (N/P_r + N/P_c) N_p}{N \times N/P_r \times N/P_c P}. \quad (6)$$

Noting that Γ is a constant, we can also reduce this formula to

$$t_{comm} \propto \frac{N_p}{P} \frac{P_r + P_c}{N}, \text{ or } t_{comm} \propto \frac{N_p}{N} \frac{P_r + P_c}{P}. \quad (7)$$

Although useful, this formula assumes both N/P_r and N/P_c are greater than Γ , which may not hold at the largest problem sizes. In particular, in our 8192^3 simulations on a 32×8192 processor grid $N/P_c = 1$, which means each

pencil is only one grid spacing wide in the z direction. Communication is then always necessary — at least to collect the required spline coefficients in the z direction for every particle. In that case, one can simply write

$$t_{comm} \propto N_p/P, \quad (8)$$

which incidentally implies perfect strong scaling, as for the computational cost t_{comp} .

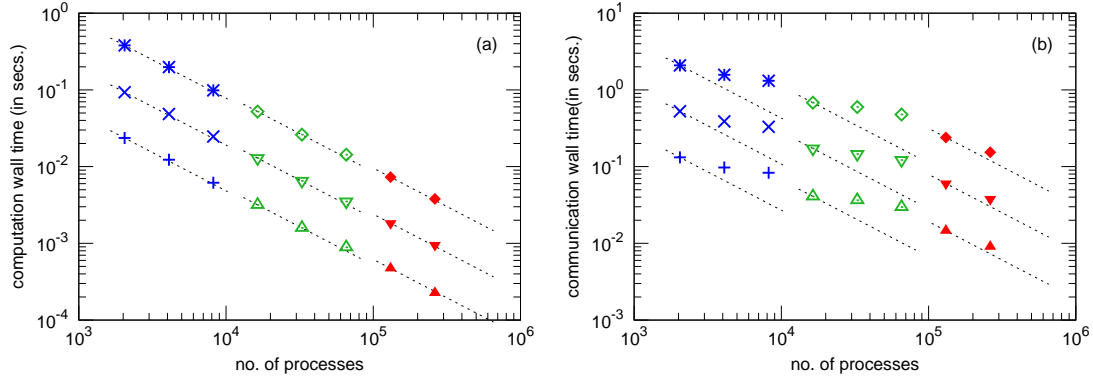


Figure 5: Breakup of (a) computational and (b) communication cost of the interpolation. Same symbols as Figure 4. Dashed lines of slope -1 represents ideal strong scaling with respect to first case of each problem size.

Figure 5 shows a scalability plot similar to that seen earlier in Fig. 4 but now for (a) computational and (b) communication times t_{comp} and t_{comm} separately. It is clear that the computation scales almost perfectly, i.e. $t_{comp} \propto N_p/P$ such that all data points with the same N_p lie virtually on the same line of slope -1, with the grid resolution having only a minor effect. Computational times for configurations with the same N_p/P , i.e. same nominal number of particles per process are also seen to agree closely. A mild increase in such timings at higher N (e.g. the dashed line for 8192^3 data points is slightly shifted upwards) is likely to be the result of increasing vector strides in arrays holding the spline coefficients accessed by the code. Some minor variations due to deviations from perfect load balancing caused by particle migrations are also expected. This latter effect is also more significant when N_p/P is reduced.

It can be seen that values of t_{comm} in Fig. 5(b) are higher than those for t_{comp} in Fig. 5(a), by an order of magnitude or more, showing that communication is still dominant over computation. This is consistent with trends in Fig. 5(b) showing a strong resemblance to those presented earlier in Fig. 4 for the total interpolation time. To analyze the communication timings more precisely in the context of (7) and (8) we present some further details including scalability percentages in Table 3. For each choice of N , strong scaling is assessed with respect to the smallest P tested for each combination with N_p also fixed, while weak scaling is assessed relative to timings obtained with P increased in proportion to N_p . It can be seen that while the strong scaling varies, weak scaling is close to perfect, which is consistent with observations that interpolation timings become almost proportional to N_p/P .

Consistent with statements in the preceding paragraphs, the numbers in Table 3 confirm that computation scales almost perfectly, and is much less expensive than communication. In this and the next paragraph we consider only data for the largest N_p tested, i.e 256M. For $N = 2048$ t_{comm} at 4K cores is 75.3% of that at 2K cores, while t_{comm} at 8K cores is 83.5% of that at 4K. This increase indicates scalability is reduced. This can be partly understood using (7) with the ratios $(P_r + P_c)/P$ being 0.0469, 0.0391 and 0.0352 at 2K, 4K and 8K cores respectively: i.e. decreasing less significantly between 4K and 8K. However, for $N = 4096$ the scalability of communication time at 64K cores relative to 32K cores is better than that of 32K cores relative to 16K cores. It is worth noting that at 64K cores the processor grid used is such that $N/P_c = 2$, which implies (7) ceases to be valid. It can also be seen that for a given N_p , improved scalability is generally obtained at larger N : e.g. t_{comm} at 16K cores (with $N = 4096$) is just 51.8% (very close to 50%) of that at 32K cores (with $N = 2048$). A similar, in fact slightly better observation can be made between t_{comm} at 128K cores (with $N = 8192$) and that at 256K cores (with $N = 4096$).

For the purpose of simulations at extreme problem sizes, the most promising observation perhaps is that, for $N = 8192$, scalability between 128K and 256K cores is significantly better than those observed at smaller problem sizes for a similar increase (doubling) of core count. It is also remarkable that this has occurred even though the

N	2048	2048	2048	4096	4096	4096	8192	8192
P	2K	4K	8K	16K	32K	64K	128K	256K
$P_r \times P_c$	32×64	32×128	32×256	32×512	32×1024	32×2048	32×4096	32×8192
16M: N_p/P	8K	4K	2K	1K	512	256	128	64
t_{comp}	0.024	0.0123	0.0062	0.0032	0.0016	0.00089	0.00047	0.00023
t_{comm}	0.132	0.0974	0.0831	0.0408	0.0365	0.0297	0.0154	0.00902
total	0.156	0.114	0.0894	0.0441	0.0380	0.0307	0.0159	0.00928
% comm	84.6%	85.4%	92.9%	92.5%	96.0%	96.7%	96.9%	97.2%
strong	–	68.4%	43.6%	–	58.0%	35.9%	–	85.7%
weak	–	–	–	–	–	–	–	–
64M: N_p/P	32K	16K	8K	4K	2K	1K	512	256
t_{comp}	0.093	0.049	0.025	0.013	0.0065	0.00035	0.0018	0.00095
t_{comm}	0.527	0.389	0.330	0.172	0.146	0.0122	0.0603	0.0379
total	0.621	0.440	0.354	0.185	0.153	0.126	0.0623	0.0389
% comm	84.9%	88.4%	93.2%	93.0%	95.4%	96.8%	96.8%	97.4%
strong	–	70.6%	43.9%	–	60.5%	36.7%	–	80.1%
weak	100.5%	103.6%	101.0%	95.5%	99.3%	97.5%	102.1%	95.4%
256M: N_p/P	128K	64K	32K	16K	8K	4K	2K	1K
t_{comp}	0.380	0.198	0.099	0.0521	0.026	0.0143	0.0073	0.0038
t_{comm}	2.089	1.573	1.314	0.680	0.598	0.477	0.240	0.154
total	2.476	1.773	1.419	0.733	0.626	0.493	0.248	0.158
% comm	84.4%	88.7%	92.6%	92.8%	95.5%	96.8%	96.8%	97.4%
strong	–	69.8%	43.6%	–	58.5%	37.2%	–	78.4%
weak	100.8%	102.9%	100.8%	96.3%	97.1%	99.6%	102.6%	94.0%

Table 3: Timings for interpolation, computational + communication and total for different problem sizes. The three tables represent particle counts of 16M, 64M and 256M. The weak scaling percentages are based on scaling up the number of particles and reporting how much of the performance is retained.

communication time accounts for some 97% of the time taken for the interpolation. Clearly, this indicates that the one-sided communication, achieved through Co-Array Fortran is itself highly efficient and scalable for our current problem configurations.

For more precise tests of the scaling estimates (7) and (8) we show in Fig. 6 communication timings (a) scaled by the factor $(P_r + P_c)/(PN)$ and (b) further divided by N_p . If Λ is the proportionality factor in (7) then the quantities being shown are ΛN_p and Λ itself respectively. If (7) holds perfectly then all data points should lie on the same horizontal line. The results suggest that (7) holds quite well at 2048^3 but there is a gradual transition to (8) as grid resolution increases to 4096^3 and 8192^3 . As mentioned earlier, this transition is partly a consequence of our practice (driven by considerations for FFT performance) of keeping P_r fixed as P is increased, which results in P_c approaching and eventually becoming equal to N at extreme problem sizes. The strong downward trend of these data points in the limit of large P suggests good scalability of the new algorithm at large core counts, as discussed above. For each problem configuration the absolute value of Λ as in frame (b) of this figure may be considered a measure of system communication performance which is inherently machine dependent.

The central characteristic of our new interpolation algorithm is that, by fetching only the spline coefficients for particles near the boundary, communication requirements are reduced to a bare minimum. This communication is also fast, being local (between adjacent MPI processes) and highly expedited via PGAS techniques implemented via Co-Array Fortran. In contrast, in the baseline algorithm before this work was conducted, every MPI process has to compute a partial sum for every particle, which involves a lot of wasteful calculations (with most contributions being zero) as well as communications. As a result, there is a huge contrast between the timings for the two approaches. While the timings for the Eulerian based operations, such as FFTs and calculation of spline coefficients are the same between two approaches, there is more than an order of magnitude difference between the interpolation operations.

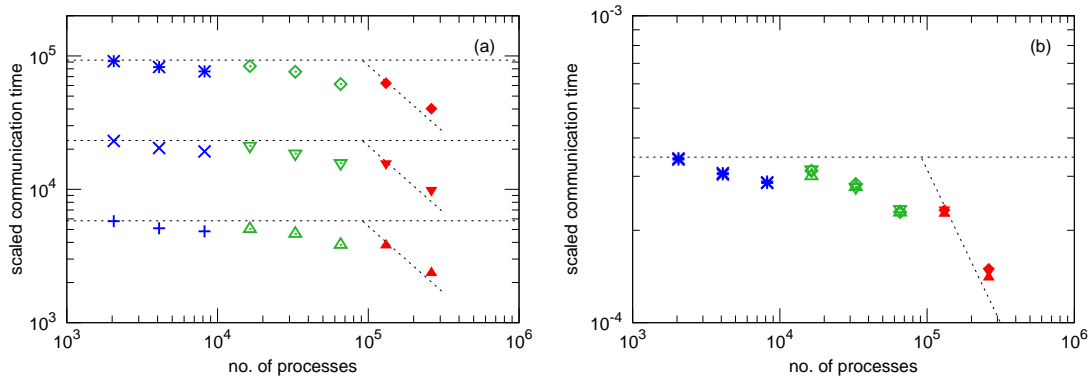


Figure 6: Scaled communication time t_{comm} divided by $(P_r + P_c)/(PN)$ in (a) and further by N_p in (b). Same symbols as Figure 4. The estimates (7) and (8) are represented by horizontal dashed lines and lines of slope -1.

For the case of $N = 8192$, $N_p = 64M$ and $P = 256K$ the original approach for interpolation (not counting the spline coefficients) takes about 18.5 seconds (Table 1), but the new approach (Table 3) takes only 0.0389 seconds. Since the cost of the interpolation increases proportionally with the number of particles, the difference in raw timings will be even greater when more particles are used. The scalability analysis presented in this section also suggests strongly that the new approach will continue to perform well at even more extreme problem sizes of N and N_p beyond the largest values tested in this work. However, it is also important to note that N_p always needs to be sufficiently less than N^3 for the current algorithm to be most viable. Since otherwise, if N_p is comparable to N^3 , the same spline coefficients would be redundantly fetched multiple times for interpolation, making a ghost layer based approach more viable.

4.3. Particle migration

The preceding discussion of communication performance has focused on the transfer of spline coefficients, which occurs for particles within a distance of up to 2 grid spacings from a sub-domain boundary. Since particles migrating to another sub-domain become the responsibility of a new host MPI process, we also consider here the cost of communication involving such particle migrations. At each Runge-Kutta sub-step, once the velocity of a particle is determined, the particle position is updated at minimal computational cost. Each MPI process then scans the positions of all particles under its control, identifying those which have just left its sub-domain. Because we use 2D decomposition, a migrating particle can potentially move to one of $3^2 - 1 = 8$ possible adjacent sub-domains. All attributes (including position and velocity information, at minimum) associated with such departing particles are copied into a temporary outgoing buffer, while the ordering of remaining particles is adjusted to fill gaps in array positions left by the departing particles. Neighboring MPI processes then exchange information on how many particles are leaving from which MPI process to which MPI process. The actual transfer of information is performed as a simple halo exchange using non-blocking `MPI_ISEND` and `MPI_IRECV` calls. Information on the arriving particles is then appended to the array holding the incumbent particles. As noted earlier, because of homogeneity in space for the turbulent flow, the number of particles in each sub-domain is almost always close to N_p/P .

Clearly, the cost of handling particle migrations is largely determined by the number of particles migrating. This number is influenced by the Courant number (C) constraint on the time step and the likelihood for particles to be located within C grid spacings of the sub-domain boundaries. For a given number of particles per process and time step, the number of particles migrating particles is also sensitive to the surface area to volume ratio of each sub-domain. In particular if a sub-domain is very thin in one direction (which happens if N/P_c is as low as 2 or 1) then considerable migration activity in that direction is expected.

Table 4 shows elapsed wall time for the particle migrations, averaged over all MPI processes and over a large number of time steps in the DNS code. A balance of competing effects leads to different trends as the core count is varied for several grid resolutions. For 2048^3 , with each doubling of core count the number of particles per process decreases by a factor of 2 while the ratio of surface area to sub-domain increases by a factor less than 2, such that the net result is a mild (less than 50%) reduction in the time spent in handling the migrations, as seen from 2K to 4K and

N	2048	2048	2048	4096	4096	4096	8192	8192
P	2K	4K	8K	16K	32K	64K	128K	256K
$P_r \times P_c$	32×64	32×128	32×256	32×512	32×1024	32×2048	32×4096	32×8192
N/P_c	32	16	8	8	4	2	2	1
% migrating	0.29%	0.48%	0.88%	0.78%	1.56%	3.13%	2.73%	5.47%
wall time	0.0041	0.0026	0.0019	0.0022	0.0020	0.0019	0.0031	0.0142

Table 4: Timings (in seconds) for operations needed to handle particle migration between different sub-domains using MPI_ISEND and MPI_RECV calls at different grid resolutions and core counts, with number of particles held fixed at 256M.

N	4096	4096	8192	8192
P	32K	32K	256K	256K
$P_r \times P_c$	32×1024	32×1024	32×8192	32×8192
N_p	64M	256M	64M	256M
Eulerian	6.59	6.59	9.20	9.20
Splines	2.33	2.33	4.42	4.42
Particles	0.31	1.25	0.08	0.32
Total	9.23	10.17	13.70	13.94

Table 5: Summary of total timings for the entire DNS code when using the dynamic particle-to-process mapping.

similarly from 4K to 8K cores. For 4096^3 , as one side of each sub-domain becomes rather thin (N/P_c falling from 8 downwards) the two effects almost mutually cancel, as a greater fraction of the N_p/P particles now reside close enough to the sub-domain boundaries for a migration to be possible. Finally, at 8192^3 , as N/P_c drops to 1, practically every particle is in a zone where migration is possible, i.e. likelihood of migration for each particle is substantially increased, leading to a substantial increase in the migration timing. It is likely that a less elongated shape of the processor grid, such as 64×4096 , with no dimension being very thin, will result in fewer migrations. However, since the time taken for migration for the largest case in the table is still well under 1% of the overall simulation time, no special strategies for further optimization of this facet of our algorithm appear to be necessary.

In regard to particle migration, we would also like to point out that the general considerations in this sub-section can change somewhat depending on the underlying flow physics or the type of particles tracked. For example, in a compressible flow, or if particle inertia is involved, local accumulations contributing to greater load imbalance (i.e., greater departure from N_p/P per MPI process) can occur. In the case of inertial particles or molecular markers with high diffusivity the particles can also move by more than one grid spacing over one time step. In such a scenario, the migration can be generalized by considering more sub-domains beyond the immediately adjacent ones, i.e., the halo-exchange is now extended to $(2n + 1)^2 - 1$ possible sub-domains (assuming 2D processor grid layout), where n is the number of neighboring sub-domains on one given side. In these situations the present algorithm is likely to be less efficient. The development of more advanced coding strategies necessary to address these further challenges is an interesting topic for future work.

4.4. Summary of overall timings

We close our performance analysis by showing in Table 5 the overall elapsed time per step for production simulations with particle tracking based on the new algorithm developed in this paper. It can be seen that the cost of interpolation is now primarily in the calculation of cubic spline coefficients from the velocity field, while the calculation of interpolated particle velocities from the spline coefficients has become highly efficient, scaling mainly with the number of particles per MPI process. The last case shown in this table shows the cost of tracking 256M particles in our largest simulation is not much more than 50% additional to the cost of computing the velocity field alone. Although the cost of following the particles does increase with N_p , we expect that most science questions on Lagrangian statistics can be answered reasonably well using particle population sizes comparable to the largest values tested in this work.

It may be recognized that there is an inevitable element of machine and hardware dependency on the numbers presented here. Clearly, our new algorithm is superior to the previous static mapping based approach. However, we are unable to make similar quantitative comparisons with other prevalent approaches based on utilizing ghost layers, due to severe memory constraints associated with them at extreme problem sizes. Nevertheless, depending on the machine hardware and interconnect along with the number of particles tracked in comparison to the number of grid points, it is possible that the ghost layer approach may become more viable. Further testing is still necessary for more definitive claims on the overall relative merits of the Co-Array Fortran and ghost layer approaches, especially on future machines with larger memory per node and improved communication bandwidth. However, since the new algorithm is based on the premise of communicating as little and as locally as possible, the general trends are likely to hold on other machines as well, provided a robust PGAS-based programming model is well supported, as it is on *Blue Waters*.

5. Conclusions

In this paper we have reported on the development of a new parallel algorithm for particle tracking in direct numerical simulations (DNS) of turbulent flow, with the objective of addressing challenges at extreme problem sizes, where a large number of fluid particles are tracked at high grid resolution on a massively parallel computer. The key task in following Lagrangian particle trajectories is to obtain the particle velocity at its instantaneous position via interpolation from a set of fixed Eulerian grid points. Cubic spline interpolation is preferred because of its high order of accuracy and differentiability [24]. From the velocity field on a periodic solution domain with N^3 grid points distributed over P parallel processes using a 2D domain decomposition (consisting of row and column communicators) $(N + 3)^3$ spline coefficients are first obtained by solving tridiagonal systems in each coordinate direction. For each particle the interpolated velocity is obtained by summing over a stencil of $4^3 = 64$ spline coefficients which may be distributed among different processes, thus requiring substantial communication. Since the particles are free to wander under the effects of turbulence, the interpolation stencil for each particle also changes continually over each time step. The existing algorithms in literature either distribute the particles among the processes in exactly the same manner at every time step or use ghost layers to incorporate information from neighboring processes. However, we find that these approaches are unable to provide acceptable performance at the largest problem sizes currently known for Eulerian-only simulations.

In this work, we have developed a new parallel algorithm where communication is reduced to a bare minimum and occurs only between processes adjacent to each other in a 2D Cartesian processor grid, thus leading to very high scalability. Particles are now distributed among the processes based on their instantaneous position, and each process is responsible for a dynamically evolving group of particles, such that all interpolation information is available either locally on the host process or its immediate neighbors. The most distinctive element of our implementation is avoiding ghost layers (which leads to high memory costs and wasteful communication) completely, in favor of one-sided communication through the use of a partitioned global address space (PGAS) programming model. In particular, we use Co-Array Fortran (CAF), which is optimal for small messages and is well-supported in the Cray Compiler Environment on the petascale supercomputer *Blue Waters* operated by the National Center for Supercomputing Applications (NCSA) at the University of Illinois, Urbana-Champaign, USA.

In our new algorithm, the spline coefficients are stored as a global co-array, which is logically partitioned into distinct sections local to each process. At the beginning of each Runge-Kutta sub-step each process decides, based on the proximity of each particle to the sub-domain boundaries, which spline coefficients need to be fetched from one or more of 8 neighboring processes. The transfer is coded as a simple CAF assignment statement whose execution is, because of local memory affinity and message size being only 4 real words, extremely fast. After this process is complete the host process performs the summation of 64 coefficients and calculates the new particle position. If a particle has moved to an adjacent domain then a halo exchange is used to transfer its information to a new host process. While these migrations occur on a regular basis the fraction of particles migrating at any one time step is generally low and hence the cost inconsequential.

Detailed benchmarking results obtained on *Blue Waters* are reported, for problem sizes from 2048^3 grid points on 2048 Cray XE cores to 8192^3 (over 0.5 trillion grid points) on 262,144 cores. The calculation of spline coefficients is slightly less efficient than 3D Fast Fourier Transforms (FFTs) which form the backbone in our simulations of velocity fields and has been optimized aggressively for our recent work [22] performed using millions of node hours on *Blue*

Waters. With spline coefficients available, the cost of the remaining interpolation operations is almost proportional to the number of particles (N_p) but also sensitive to the Eulerian problem size (N) and the shape ($P_r \times P_c = P$) of the 2D domain decomposition used for the latter. These particle costs are dominated by communication which is especially sensitive to the shortest dimension of each sub-domain compared to the size of the interpolation stencil in each direction. Both theoretical arguments and actual performance data (Figs. 4 and 5) indicate, somewhat counter-intuitively, that the scalability of this algorithm actually improves with increasing problem size. For our 8192^3 simulation with 256M particles the performance improvement obtained (see contrast between Tables 1 and 5) is so substantial that the fraction of additional time for tracking 256M particles compared with an Eulerian simulation is only about 50%, which is less than the corresponding fractional cost for 16M particles in a 2048^3 simulation.

In summary, in the work described in this paper we have successfully overcome a challenge in scalability for tracking a large number of fluid particles in a spatial solution domain which is distributed over a large number of parallel processes. The key is to aggressively minimize communication, which is implemented using Co-Array Fortran (CAF) based on a partitioned global address space (PGAS) programming model. Use of CAF is especially advantageous in our application because the algorithm uses small although numerous messages and is localized between immediately neighboring processes.

Some of the conclusions of this paper may be partly dependent on machine architecture, including the network characteristics of *Blue Waters*. However, since CAF is part of the Fortran 2008 standard, the applicability of our CAF-based algorithm on other major platforms is expected to increase in the future.

Acknowledgments

This research is part of the Blue Waters sustained-petascale computing project, which is supported by the National Science Foundation (NSF) awards OCI-0725070 and ACI-1238993 and the state of Illinois. Blue Waters is a joint effort of the University of Illinois at Urbana-Champaign and National Center for Supercomputing Applications (NCSA). The authors gratefully acknowledge support from NSF, via Grant ACI-1036070 (from the Petascale Resource Allocations Program) which provided access to Blue Waters and Grant CBET-1235906 (from the Fluid Dynamics Program) which provided the scientific impetus for this research. We thank Dr. R.A. Fiedler of Cray Inc. for his advice on use of Co-Array Fortran, staff members of the Blue Waters project for their valuable assistance, and K. Ravikumar at Georgia Tech for his help with the contents of Tables 1 and 4. In addition, we are grateful to anonymous referees for their constructive comments which have helped improve the manuscript further.

References

- [1] F. Pasquilli, F. B. Smith, Atmospheric diffusion, Ellis Horwood, Chichester, U.K., 1983.
- [2] R. A. Shaw, Annu. Rev. Fluid Mech. 35 (2003) 183–227.
- [3] S. B. Pope, Progr. Energy Combust. Sci. 11 (1985) 119–192.
- [4] S. Elghobashi, Appl. Sci. Res. 52 (1994) 309–329.
- [5] L. Biferale, F. Bonaccorso, I. M. Mazzitelli, M. A. T. van Hinsberg, A. S. Lanotte, S. Musacchio, P. Perlekar, F. Toschi, Phys. Rev. X 6 (2016) 041036.
- [6] P. G. Saffman, J. Fluid Mech. 8 (1960) 273–283.
- [7] B. L. Sawford, J. C. R. Hunt, J. Fluid Mech. 165 (1986) 373–400.
- [8] A. S. Monin, A. M. Yaglom, Statistical Fluid Mechanics, Vol. 1, MIT Press, 1971.
- [9] A. S. Monin, A. M. Yaglom, Statistical Fluid Mechanics, Vol. 2, MIT Press, 1975.
- [10] B. L. Sawford, J.-F. Pinton, Ten Chapters in Turbulence, Cambridge University Press, 2013.
- [11] S. B. Pope, Annu. Rev. Fluid Mech. 26 (1994) 23–63.
- [12] B. L. Sawford, Annu. Rev. Fluid Mech. 33 (2001) 289–317.
- [13] P. K. Yeung, Annu. Rev. Fluid Mech. 34 (2002) 115–142.
- [14] F. Toschi, E. Bodenschatz, Annu. Rev. Fluid Mech. 41 (2009) 375–404.
- [15] J. P. L. C. Salazar, L. R. Collins, Annu. Rev. Fluid Mech. 41 (2009) 405–432.
- [16] S. Balachandar, J. K. Eaton, Annu. Rev. Fluid Mech. 42 (2010) 111–133.
- [17] P. Moin, K. Mahesh, Annu. Rev. Fluid Mech. 30 (1998) 539–578.
- [18] T. Ishihara, T. Gotoh, Y. Kaneda, Annu. Rev. Fluid Mech. 41 (2009) 165–180.
- [19] M. Yokokawa, T. Itakura, A. Uno, T. Ishihara, Y. Kaneda, Proceedings of the Supercomputing Conference, Baltimore, 2002.
- [20] M. Lee, N. Malaya, R. D. Moser, Proceedings of the International Conference on High Performance Computing, Networking, Storage and Analysis, SC '13, ACM, Denver, CO, 2013
- [21] S. B. Pope, Turbulent Flows, Cambridge University Press, Cambridge, U.K., 2000.

- [22] P. K. Yeung, X. M. Zhai, K. R. Sreenivasan, *Proc. Nat. Acad. Sci.* 112 (2015) 12633–12638.
- [23] T. Ishihara, K. Morishita, M. Yokokawa, A. Uno, Y. Kaneda, *Phys. Rev. Fluids* 1 (2016) 082403.
- [24] P. K. Yeung, S. B. Pope, *J. Comput. Phys.* 79 (1988) 373–416.
- [25] S. Balachandar, M. R. Maxey, *J. Comput. Phys.* 83 (1989) 96–125.
- [26] H. Homann, J. Dreher, R. Grauer, *Comput. Phys. Comm.* 117 (2007) 560–565.
- [27] D. Buaria, P. K. Yeung, *Proceedings of the 2014 Annual Conference on Extreme Science and Engineering Discovery Environment, XSEDE '14*, ACM, Atlanta, GA, 2014
- [28] D. Buaria, B. L. Sawford, P. K. Yeung, *Phys. Fluids* 27 (2015) 105101.
- [29] D. Buaria, P. K. Yeung, B. L. Sawford, *J. Fluid Mech.* 799 (2016) 352–382.
- [30] S. Plimpton, *J. Comput. Phys.* 117 (1995) 1–19.
- [31] J. C. Phillips, R. Braun, W. Wang, J. Gumbart, E. Tajkhorshid, E. Villa, C. Chipot, R. D. Skeel, L. Kale, K. Schulten, *J. Comput. Chem.* 26 (2005) 1781–1802.
- [32] P. J. Ireland, T. Vaithianathan, P. S. Sukheswalla, B. Ray, L. R. Collins, *Comput. Fluids* 76 (2013) 170–177.
- [33] O. Ayala, H. Parishani, L. Chen, B. Rosa, L.-P. Wang, *Comput. Phys. Comm.* 185 (2014) 3269 – 3290.
- [34] R. W. Numrich, J. Reid, *SIGPLAN Fortran Forum* 17 (1998) 1–31.
- [35] V. Eswaran, S. B. Pope, *Comput. Fluids* 16 (1988) 257–278.
- [36] D. A. Donzis, P. K. Yeung, *Physica D* 239 (2010) 1278–1287.
- [37] R. S. Rogallo, *NASA Technical Memo 81315*, NASA Ames Research Center.
- [38] C. Canuto, M. Y. Hussaini, A. Quarteroni, T. A. Zang, *Spectral Methods in Fluid Dynamics*, Springer-Verlag, 1988.
- [39] G. S. Patterson, S. A. Orszag, *Phys. Fluids* 14 (1971) 2538–2541.
- [40] D. A. Donzis, P. K. Yeung, D. Pekurovsky, *Proc. TeraGrid '08 Conf.*, Las Vegas, NV, 2008.
- [41] P. D. Mininni, D. Rosenberg, R. Reddy, A. Pouquet, *Parallel Comput.* 37 (2011) 316 – 326.
- [42] D. Pekurovsky, *SIAM J. Sci. Comput.* 34 (2012) C192–C209.
- [43] O. Ayala, L.-P. Wang, *Parallel Comput.* 39 (2013) 58 – 77.
- [44] R. A. Fiedler, N. Wichmann, S. Whalen, D. Pekurovsky, *Cray User Group Proc.*, Napa Valley, CA, 2013.
- [45] R. Gerstenberger, M. Besta, T. Hoefler, *Proceedings of the International Conference on High Performance Computing, Networking, Storage and Analysis, SC '13*, ACM, Denver, CO, 2013
- [46] R. Nishtala, Y. Zheng, P. H. Hargrove, K. A. Yelick, *Parallel Comput.* 37 (2011) 576–591.
- [47] P. K. Yeung, *J. Fluid Mech.* 427 (2001) 241–274.
- [48] C. Meneveau, *Annu. Rev. Fluid Mech.* 43 (2011) 219–245.
- [49] B. L. Sawford, P. K. Yeung, M. S. Borgas, P. Vedula, A. LaPorta, A. M. Crawford, E. Bodenschatz, *Phys. Fluids* 15 (2003)
- [50] P. K. Yeung, S. B. Pope, E. A. Kurth, A. G. J. *Fluid Mech.* 582 (2007) 399–422.
- [51] J. H. Ahlberg, E. N. Wilson, J. L. Walsh, *The Theory of Splines and Their Applications*, Academic Press, 1967.
- [52] C. Teijeiro, G. Sutmann, G. Taboada, J. Touriño, *Comput. Phys. Comm.* 184 (2013) 1191 – 1202.
- [53] M. P. Clay, D. Buaria, T. Gotoh, P. K. Yeung, *Comput. Phys. Comm.* (2017) (published online, <http://dx.doi.org/10.1016/j.cpc.2017.06.009>).